TEST Engineering & Management

July - August 2020
ISSN: 0193-4120 Page No. 3624 - 3636

Experimental Study on Elastoplastic Static Behavior of Steel-Concrete Composite Hollow Sandwich Plate

Jing Chen[1], Kejian Ma[1,2], Jianchun Xiao[1,2], Yanhui Wei[1,2*], Hongniao Chen[1], Yaqin Lu[1]

[1] Space Structures Research Center, Guizhou, Guiyang, China

[2] Guizhou Key Laboratory of Structural Engineering, Guizhou, Guiyang, China

Corresponding Author's Email: yhwei@gzu.edu.cn

Article Info Volume 83
Page Number: 3624 - 3636
Publication Issue:
July - August 2020

Article History
Article Received: *25 April 2020*
Revised: *29 May 2020*
Accepted: *20 June 2020*
Publication: *10 August 2020*

Abstract

This paper took steel-concrete composite hollow sandwich plate as the research object, built a full-size test model to test the elastoplastic static behavior, and obtained the structure deformation and failure mechanism of steel-concrete composite hollow sandwich plate. The crack development and distribution on concrete pavement were observed, which provides a basis for the design and promotion of steel-concrete composite hollow sandwich plate. On the basis of test, the finite element software was adopted to simulate and analyze the test process. The results show that the steel-concrete composite hollow sandwich plate has enough elastoplastic bearing capacity, and the overall deformation displays a bowl shape, similar to that of traditional floor. From the failure test, it is found that the shear key of steel tube at the support is obviously deformed by tension and compression, the upper and lower chord of side-span steel show buckling failure, and the cracks of surface concrete plate mainly concentrate on the top surface near support attachments. The finite element simulation was used, and the results are well identical with test results. The proposed finite element parameter can simulate the real force on steel-concrete composite hollow sandwich plate.

Keywords: Steel-concrete Composite Hollow Sandwich Plate, Full-size Test Model, Ultimate Bearing Test, Finite Element Simulation

1. INTRODUCTION

Steel-concrete composite hollow sandwich plate is composed of surface concrete plate and crossed steel hollow beams. The basic structure of steel hollow beams is composed by T section steel upper and lower chords and the shear connectors of square steel tube, as shown in Fig.1a. The surface concrete plate is connected with T section steel upper chord through studs, to compose the steel-concrete composite hollow sandwich plate as shown in Fig.1b.

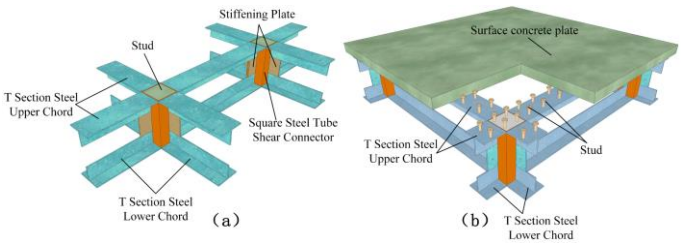

July - August 2020
ISSN: 0193-4120 Page No. 3624 - 3636

Fig.1 Schematic diagram of the structure of steel-concrete composite hollow sandwich plate

Fig.2 is the schematic diagram of the dimensions of steel-concrete composite hollow sandwich plate. The steel grid hollow sandwich plate can be deemed as "a plate having shear deformation" [1]. The thickness of the steel-concrete composite hollow sandwich plate is h=(1/25~1/30) l(l is the structural short span size). b is the thickness of surface reinforced concrete floor, which should not be less than 80mm; h_1 is the height of upper and lower chord T section steel, h_2 is the hollow height of hollow sandwich plate; the width of rectangular tube shear connector is the same as the flange width of upper and lower chord T section steel, so does the thickness; a_1 is the width of stiffening plate, a_2 is the width of shear connector. The ratio of the total width a of shear connector and stiffening plate and the hollow height h_2 of hollow sandwich plate is larger than 1 (a/h_2＞1). Only if this condition is met, the shear connector node can be regarded as the stress component mainly subject to shear deformation in the design [2]. In order to ensure that the steel-concrete composite hollow sandwich plate has the mechanical property of grid plate, the short-span grid number of sandwich plate shall be larger than 5 [3], and the single grid dimension la is between 2.5~3.5 m and should be no more than 4 m.

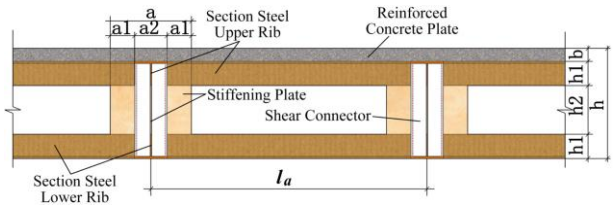

Fig.2 Schematic diagram of steel-concrete composite hollow sandwich plate dimension

The steel-concrete composite hollow sandwich plate has the mechanical property of spatial plate, such as three-dimensional stress, light structural weight and large rigidity, which has been applied in multiple projects and achieved great social economic effect [4]. A field test of the steel-concrete composite hollow sandwich plate system was carried out in combination with real project. Literature [5] conducted a local overload test of the steel hollow sandwich floor of a completed 21 m-span multi-story factory building, and the results show that under the effect of 1.5 times of designed load, the floor is still in a elastic range (Fig.3); Literature [6] made a comfort analysis and experimental research of 19 m-span steel-concrete composite hollow sandwich plate floor, and the research indicates that the steel-concrete composite hollow sandwich plate can take into consideration of both safety and comfort(Fig.4). Most recent studies focus on the steel-concrete composite hollow sandwich plate in elastic stress stage, but the research on the elastoplastic stage of steel-concrete composite hollow sandwich plate, especially the experimental research, is rarely reported. Based on this, the paper used a full-scale test model of steel-concrete composite hollow sandwich plate to carry out a ultimate load test and study the structural deformation and failure mechanism of steel-concrete composite hollow sandwich plate, and adopted the finite element software to simulate the test process and verify the test results.

Fig.3 Local overload field test of an industrial factory building

July - August 2020
ISSN: 0193-4120 Page No. 3624 - 3636

Fig.4 A field test on the comfort of an industrial factory building

2. EXPERIMENTAL PLANS ON THE ELASTOPLASTIC STATIC PROPERTY OF STEEL-CONCRETE COMPOSITE HOLLOW SANDWICH PLATE

2.1 Design of test structural model

This test adopted the full-scale model of orthogonal positively-placed steel-concrete composite hollow sandwich plate [7], with grid spacing of 1.5 m. In order to guarantee the model has the mechanical properties of the plate, there are 5 grids in both X and Y directions, the overall dimension of model plane is 7.5 m by 7.5 m, the model plane and axis side are shown in Fig.5. The height of steel-concrete composite hollow sandwich plate is 250 mm. The upper chord T section steel flange was set with a single row of studs with diameter of 16 mm, spacing at 100 mm. The top was poured with 80 mm thickness of reinforced concrete plate. The cross section of the upper and lower rib of hollow sandwich plate is T-section steel, and the cross section of shear connector is square steel tube. The thickness of upper and lower blanking plate of shear connector is 9 mm, and the blanking plate top parallels with the T section steel flange of upper and lower ribs. Since the hollow height of hollow sandwich plate is only 125 mm, considering the convenience in processing model, no stiffening plate was set around the shear connector.

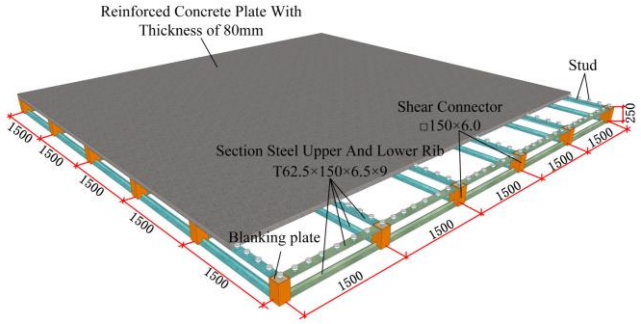

Fig.5 Dimensional Diagram of Steel-Concrete Composite Hollow Sandwich Plate

The steel-concrete composite hollow sandwich plate model was hoisted on a reinforced concrete frame structure pedestal of 1.5 m height, for the convenience of model loading and data observation. The schematic diagram of pedestal is shown in Fig.6. Rigid gaskets were set at the corresponding positions of support frame beam of steel-concrete composite hollow sandwich plate, as the support of steel-concrete composite hollow sandwich plate. Fig.7 is the schematic diagram of test model.

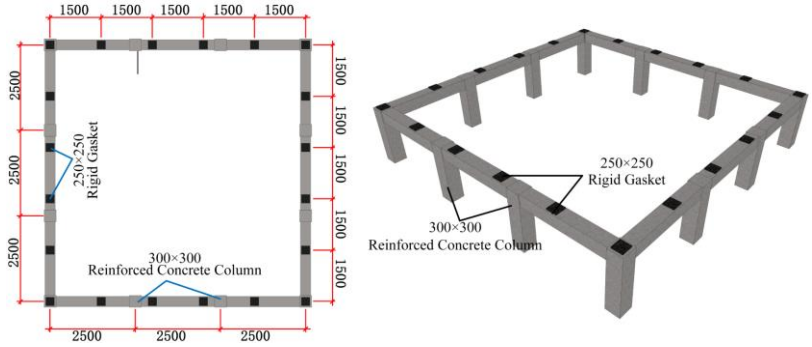

Fig.6 Schematic diagram of reinforced concrete frame pedestal

July - August 2020
ISSN: 0193-4120 Page No. 3624 - 3636

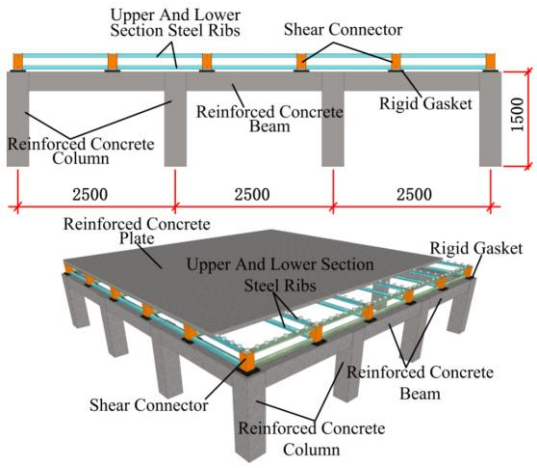

Fig.7 Schematic diagram of test model

2.2 Static loading plan

The elastoplastic static property test of steel-concrete composite hollow sandwich plate utilized sandbag and casting pig to simulate the vertical even load [8]. Each sandbag weighs 0.35 KN, and the equivalent distributed load of one layer of sandbags is about 1.5 KN/m^2. The dimension of each casting pig is 200×200×50 (L×W×H, unit: mm), with unit weight of 0.14 KN, and the equivalent distributed load of one layer of casting pigs is about 2.0 KN/m^2. In this test, the ultimate load of the test model is about 17 KN/m^2, and in the whole loading process, 6 layers of sandbags (12KN/m^2) and 4 layers of casting pigs (5KN/m^2) were to be forced. Fig.8 shows the field loading photos.

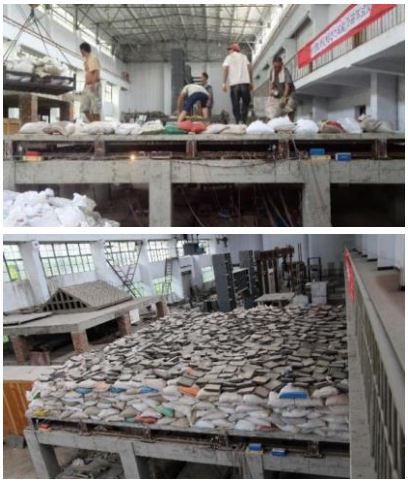

Fig.8 Loading photos shot in test field

First, the test model was divided into three levels for pre-loading test. 1.5 KN/m^2 was loaded at each level, then unloaded until loading to 4.5 KN/m^2 (design load), and the monitoring equipment was in normal operation. This test was divided into 12 levels of loading. Each level of loading was the same as pre-loading condition, i.e. 1.5KN/m^2, and finally added to 17KN/m^2. The time of loading at each level was controlled within half an hour. Then, let it stand still for half an hour. Later, observed the deformation, stress and crack development condition under each level of loading. The whole loading process shall continue for 2 days. Fig.9 shows the schematic diagram of test loading steps.

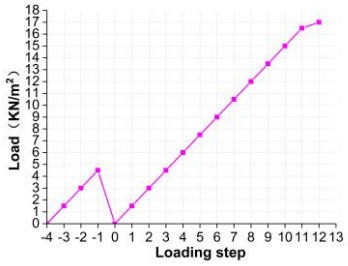

Fig.9 Schematic diagram of test loading steps

2.3 Test monitoring plan

Fixed six displacement meters (DTs-) at the bottom of steel grid hollow sandwich plate, and measured the deflection of corresponding monitoring points of steel-concrete composite hollow sandwich plate at each level of loading process; set strain gauges at the key positions of upper and lower chord section steel, and collected strain data of these positions in the loading process. Fig.10 is the layout plan of displacement meter and strain gauges. Taking structural symmetry into consideration, the measure points mainly focused on one side of test model, and several point locations on the other side were selected as check points. Four strain gauges were arranged at the corresponding positions of upper and lower chord ends (near shear connector) of each grid and the midspan. For example, A1 and A2 represent the strain gauges at the upper chord of hollow sandwich plate beam-1, and the strain of

TEST Engineering & Management

July - August 2020
ISSN: 0193-4120 Page No. 3624 - 3636

upper chord type steel flange and web are measured, respectively; A3 and A4 represent the strain gauges at the lower chord of hollow sandwich plate beam-1, and the strain of lower chord type steel web and flange are measured, respectively. J1, J2 and J3 represent the strain gauges at the upper, middle and lower positions of shear connector.

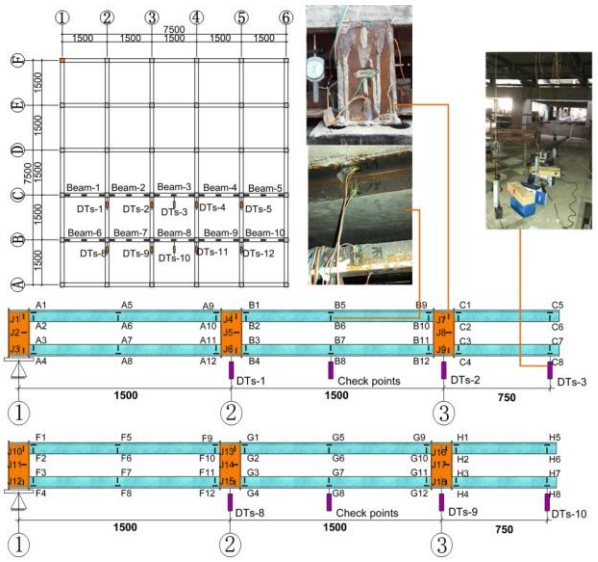

Fig.10 Layout of strain gauges and displacement meter

2.4 Steel and concrete properties test

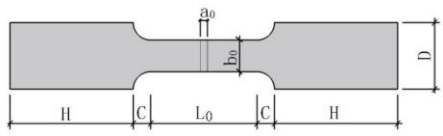

Fig.11 Schematic diagram of steel tensile sample

The test model steel is Q235B. Before the test, the steel material received a uniaxial tensile properties test [9]. The following properties of steel used in test model were tested: elasticity modulus(E), elongation(δ), yield strength(f_y), tensile strength (f_u), etc. Fig.11 is the schematic diagram of steel tensile sample. Test base metals were selected from the T section steel flange,web and square steel tube of machining model respectively, to process into three groups of test standard specimen. The material strength of test concrete was C30. The concrete properties test mainly focused on the compressive strength of concrete base material. Totally, three groups of 150 mm cubic standard specimen were manufactured and maintained in standard conditions for 28d, and then received compressive strength test [10,11]. The test results of steel and concrete properties are shown in Table 1. Steel properties test and Table 2. Concrete properties test.

Table 1

Steel properties test

Parameters	S-1	S-2	S-3
H（mm）	150	150	150
C（mm）	20	20	20
L0（mm）	90	70	90
a0（mm）	13	9	8
b0（mm）	25	20	25
D（mm）	50	50	50
fy（Mpa）	256	273	241
fu (Mpa)	315	321	298
δ(%)	27	24	29
E(Mpa)	2.03e5	2.05e5	2.05e5
fy/fu	1.42	1.36	1.41

Table 2

Concrete properties test

Strength grade	Specimen dimension(mm)	Specimen No.	Compressive strength
C30	150×150×150	W-1	36.5 36.0 40.6

3. TEST MONITORING RESULTS

3.1 Concrete crack development and steel component failure monitoring

During the first four levels of loading with load reaching to 6 KN/m^2, the reinforced concrete pavement was carefully monitored, and no evident

July - August 2020
ISSN: 0193-4120 Page No. 3624 - 3636

crack was found on the top surface of concrete plate. In this course, neither the beam nor the weld joints failed, the contact surface between the concrete plate and the upper chord of hollow sandwich plate did not show peeling phenomenon, and no steel-concrete slippage phenomenon was observed between the upper chord type steel flange and concrete. This demonstrates that under the such load effect, the reinforced concrete pavement still cooperates and jointly bears load with the lower crossed hollow beam. When the load reaches to about 7.5 KN/m^2, the concrete shows the first shearing crack which is mainly located at the ends of concrete plate pavement and steel hollow beam side. After standing still for half an hour, the width of this crack extends to 2.5~5.0 mm, as shown in Fig.12a. At this time, the pure bending area of concrete plate at the bottom of middle grid displays tensile crack, and the lower surface of shear connector concrete corner also show a crack, as shown in Fig.12b.

(a)Warping crack of concrete plate at shear connector side (b)Bottom crack of concrete plate at shear connector corner

Fig.12 Photos of crack development on concrete plate

With the increased load, the cracks continued to expand. When the load was increased to 17 KN/m^2, the structure still did not collapse, but a large area of concrete floor bottom showed tiny cracks, and the crack of concrete plate at side-span support that was connected to shear connected was larger. However, no obvious crack was found on concrete plate surface at hollow sandwich plate mid-span. After unloaded, the distribution diagram of cracks on the concrete plate surface of hollow sandwich plate was drawn, as shown in Fig.13. Due to the larger tensile stress generating from warping of simple support, the cracks on concrete plate surface mainly concentrated on shear connector support, showing symmetry.

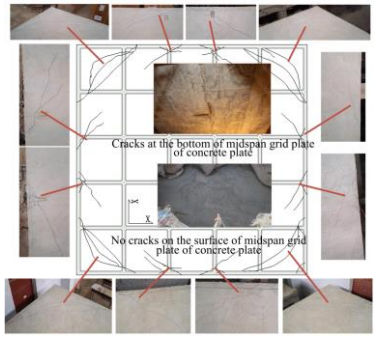

Fig.13 Distribution of cracks on concrete plate surface of hollow sandwich plate

3.2 Deflection monitoring of steel-concrete composite hollow sandwich plate

The vertical deflection of monitor points of test model under different loading steps are shown in Fig.14. Fig.14a and 14b show the deflections of C-axis and B-axis monitor points of hollow sandwich plate model under test load effect. The monitor points on both axis have the same deformation characteristics, and the C-axis deflection is about two time of B-axis deflection. The deflection shows a bowl shape, and the maximum deflection appears in the midspan position and gradually diminishes from midspan to pedestal direction, with a typical deformation characteristics of plate. When the applied load reaches to 4.5 KN/m^2, the defection at the test monitor point 3 is the maximum, and the monitoring value is 15.4mm, that's the 1/487 of the span. Under the design load effect, it is specified in the Code for Design of Steel Structure that the structure's vertical deflection shall be 1/400(18.8 mm) of the span, so that the test model can meet the requirements [12]. When the load reaches to 10 KN/m^2, the deflection at monitor points of C-axis shows great change compared to the monitoring value of previous level. When the load reaches to 17 KN/m^2, the midspan deflection of test model is 1/82(91.1 mm) of the span, and the structure has entered in a yield stage but still does not collapse.

TEST Engineering & Management
July - August 2020
ISSN: 0193-4120 Page No. 3624 - 3636

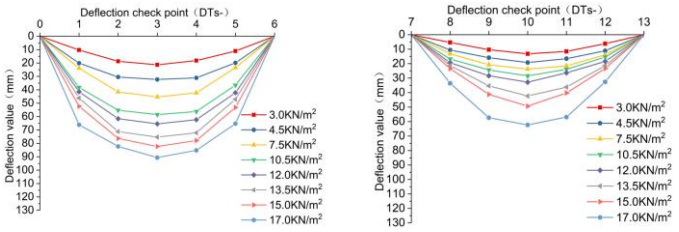

Fig.14 Vertical deflection at monitor points of model under test load

3.3 Failure of upper and lower chord of steel-concrete composite hollow sandwich plate

In the process of test, when the test load exceeded the design load (6.0KN/m^2), as the load increased, the hollow sandwich plate hollow beam generated slight sound. When the uniform load reached to 12KN/m^2, the hollow sandwich plate dramatically declined and generated great vertical deformation, with deflection of midspan being far more than that at the monitor points near the pedestal. Assuming that in the loading process, that the steel components produce sound represents that the hollow beam starts to yield (in the process of standing still, no weld joint failure was found in exterior detection). On this basis, the width of chamfer crack on concrete side is expanded(12a), at this time, the vertical deflection of steel-concrete composite hollow sandwich plate model increases quickly, the upper and lower chord T section steel close to the first grid of shear connector shows tensile and compressive yield, and the shear connectors of pedestal have obvious tensile and compressive deformation. Fig.15 is the schematic diagram of steel component failure.

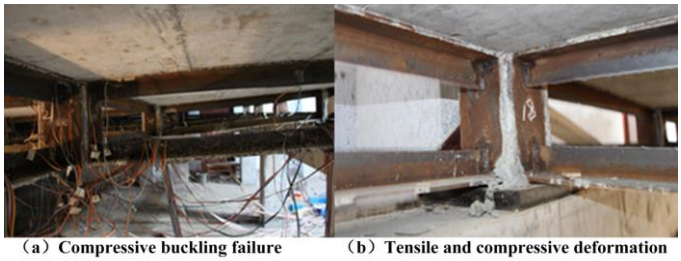

Fig.15 Failed steel components of hollow sandwich plate

3.4 Monitoring of component strain of steel-concrete composite hollow sandwich plate components

Fig.16 shows the strain at monitor points of upper and lower chord bar of hollow beam. The diagrams record the strain at C-axis and B-axis monitor points in test model in different loading steps. In the diagram, zero marks that the left are the monitor points at upper chord bar of corresponding grid of the model, and the right are the monitor points at lower chord bar of corresponding grid of the model, both of which are basically consistent in their strain development tendency. In the initial stage, the strain shows an approximately linear growth with the loading step, indicating that the structure is in the elastic stage. At the fifth loading step, the stain of some monitor points decreases after a leaping increase, suggesting that these monitor points enter in the plastic stage and produce stress redistribution. It can be seen from the diagram that most yield points at upper and lower chord bar approach the monitor point location of shear connector, the yield points at upper chord section steel are located at the web, and both lower chord section steel web and flange have yield points. At the same position, the strain monitor values of the monitor points at the lower chord section steel of hollow beam are larger than those of upper chord section steel. This phenomenon appears due to the declining stress on upper chord section steel flange caused by a combined action between the upper chord section steel flange of hollow beam and the concrete pavement.

July - August 2020
ISSN: 0193-4120 Page No. 3624 - 3636

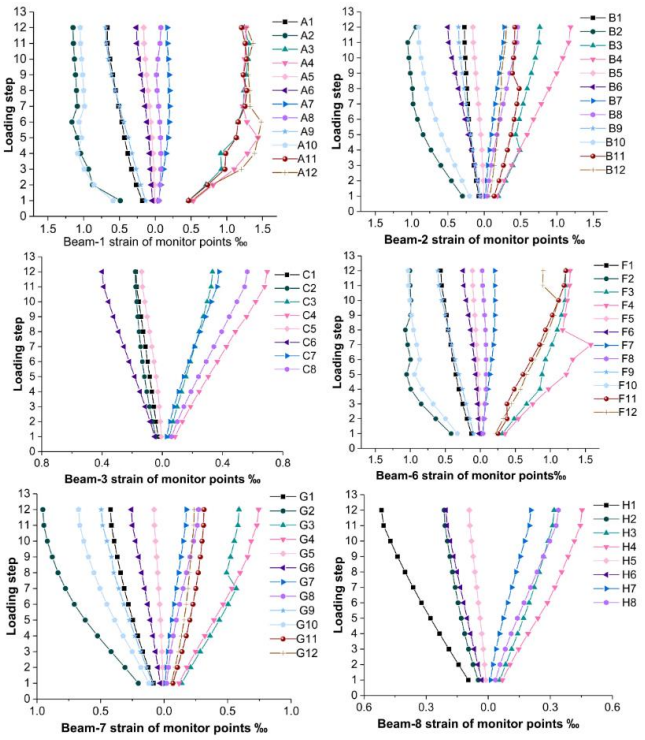

Fig.16 Strain of monitor points at upper and lower ribs of hollow beam

Fig.17 shows the strain value of monitor points at shear connector. Due to the existence of concrete pavement, the axial compressive force, shear force and local bending moment have little impact on the upper chord of hollow sandwich plate. So, the strain of monitor points at upper part of shear connector is less than that at lower part, and the strain of monitor points in the middle of the same shear connector is the minimum. It can be observed from the diagrams that the monitor points at lower part of shear connector J3, J8 and J15 are significantly larger than other monitor points, and their strain curves display the yield phenomenon.

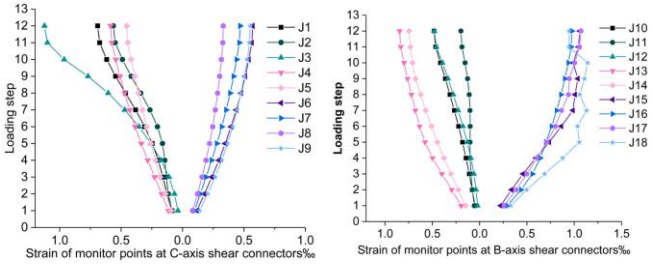

Fig.17 Strain of monitor points at shear connectors of hollow beam

4. FINITE ELEMENT SIMULATION AND TEST RESULT COMPARISON

4.1 Establishment of finite element model

The finite element software was adopted to simulate the test model, analyzed and compared the test monitor data, and verified the test phenomenon. In the finite element simulation software, all steel components were simulated using solid element (solid45). The 80mm thick concrete pavement of 300 mm by 300 mm at the top of shear connector used solid element(solid45) [13]. In order to simplify the calculation, the concrete plate in the rest range used the shell element(shell63) with bending and thin film properties. The contact between concrete solid element and shell element is set as conode, and the contact between concrete plate and hollow beam pavement is set as stationary contact (without consideration of the slippage coefficient of stud and concrete [14]). Fig.18 is the schematic diagram of a part of finite element model.

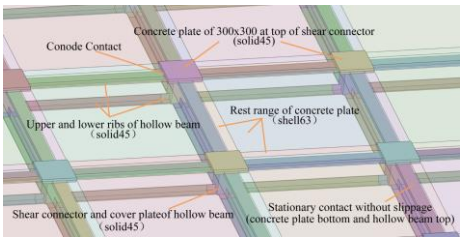

Fig.18 Schematic diagram of a part of finite element model

The steel hollow beam uses structural nonlinear steel(Structural Steel NL), which Young modulus is 2.1×10^5 MPa, density is 7850 kg/m^3 and Poisson's ratio is 0.3. Fig.19 shows the stress-strain curves under an ideal state of steel. Supposing that its yield tress is 235 MPa and ultimate strain is 0.15, and ignoring the steel hardening stage, the steel material is simplified as an ideal elastoplastic material [15]. When the steel reaches to the yield point, the steel strain can achieve 2~3%. Under so great deformation, it is considered that the structure reaches to the failure point and can not bear any more load.

July - August 2020
ISSN: 0193-4120 Page No. 3624 - 3636

The concrete plate uses nonlinear concrete material (Concrete NL), which elastic modulus is 3.0×10^4 MPa, density is 2500 kg/m^3 and Poisson's ratio is 0.18. The strain rate of concrete under compressive state is lower, so it is considered as a elastoplastic material [16], and the ultimate compressive strength of concrete in finite element model is set as 37.4 MPa.

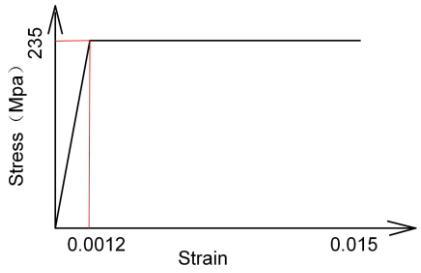

Fig.19 The stress-strain curve under ideal steel state in finite element model

In the full scale model, the concrete plate and steel hollow beam are connected by studs. In finite element model, in order to simplify calculation, the interface between the concrete plate simulated by shell element(shell63) and the solid hollow beam(solid45) are bonded using non-slippage stationary contact, and the contact surface between solid concrete plate element(solid45) and solid hollow beam(solid45) is bonded using conode [17]. Ignoring the influence of manual work on the mechanical behavior of hollow sandwich plate in the loading process, the dead load of hollow sandwich plate model was considered by setting a vertical weight accelerated speed. Fig.20 is the schematic diagram of grid division of finite element model.

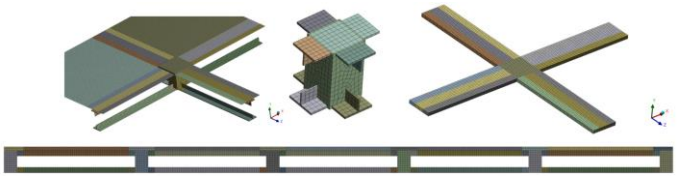

Fig.20 Schematic diagram of grid division of finite element model

4.2 Analysis of computation results of finite element

Fig.21 shows the vertical displacement cloud diagram of the structure simulated by finite computation model after loading is finished. It can be seen from the displacement cloud diagram that, the vertical displacement of hollow sandwich plate gradually increases from pedestal to midspan, and the maximum vertical displacement is at midspan, with a value of 85.615 mm (85.615/7500 of the span=1/88). The test monitor data is 91.1 mm (i.e. 91.1/7500 of the span=1/82), which is 6.4% more than finite element simulated value. The concrete plate at the top of pedestal produced upward warping deformation of 2 mm. In the test process, it can be observed from this position that, the transverse crack generated due to warping deformation (Fig.12a), and this coincides with the actual compressive deformation. In the diagram, the upper concrete plate and lower steel hollow beam of the hollow sandwich plate display compatible deformation, producing bowl-shape vertical deformation, and the vertical deflection value decreases from midspan to pedestal. This structure has the deformation effect of plate, and the finite element simulation is consistent with the test monitor data.

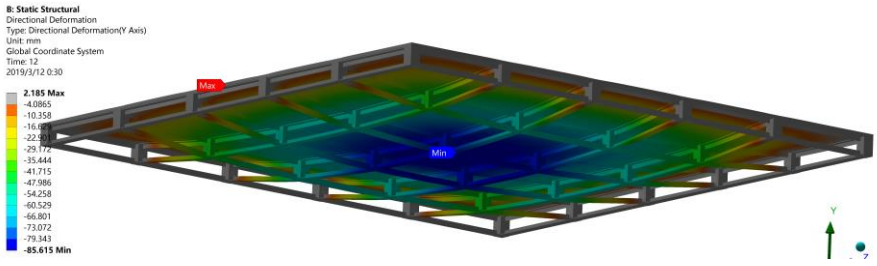

Fig.21 Vertical displacement cloud diagram after the finite element model is loaded

July - August 2020
ISSN: 0193-4120 Page No. 3624 - 3636

In the finite element computation model, the check point location of C axis and D axis of test model were selected, the computation results were extracted, the vertical displacement curves of corresponding loading step were drawn, and the test monitor data was compared, as shown in Fig.22. It can be seen from the comparison diagrams that, the change tendency of the finite element computation data is the same with that of the deflection data at test monitor points, but the actual test values are larger than the finite element simulation data. In the loading step of 4.5 KN/m^2, the test monitor value is similar to the finite element computation value; when the load reaches to 12 KN/m^2 and 17 KN/m^2, there is a large difference between test measured data and finite element computation deflection. In addition to measuring error, there are two main reasons: 1. the finite element model sets the concrete bottom surface and hollow beam contact surface as non-slippage stationary constraint, and in fact, both of them are bonded by and transit force through studs. With increased load, the concrete wrapping around studs will suffer from destroy and inevitably result in greater deflection of hollow sandwich plate; 2. in the finite element model, the steel structure uses elastoplastic material under an ideal state. Ignoring the hardening stage, when the load increases to a ultimate load of 235MPa, the material failure would not generate strain, which is slightly different from the compression on test model [18].

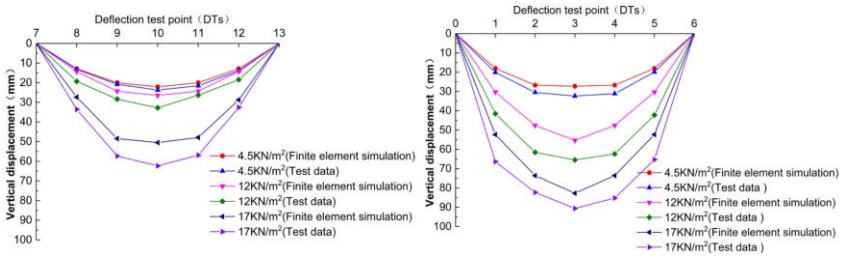

Fig.22 Comparison of finite element simulation and test deflection

Fig.23 shows the cloud diagram of side-span component with equivalent stress at the third loading step(4.5 KN/m^2) of lower steel hollow beam, with the maximum stress of 344.28 MPa. This stress is mainly caused by the stress at the connected nodes of lower chord T section steel web terminal and shear connector. The stress at upper and lower chord T section steel near the shear connector web position is 221.32 MPa (green area in the diagram), approximating to the yield stress (235 MPa). It can be seen from the diagram that the upper and lower chord section steel of the first grid near pedestal has obvious deformation characteristics: upper chord T section steel is deformed by tension, and lower chord T section steel is deformed by compression. This conforms to the deformation phenomenon observed in the test.

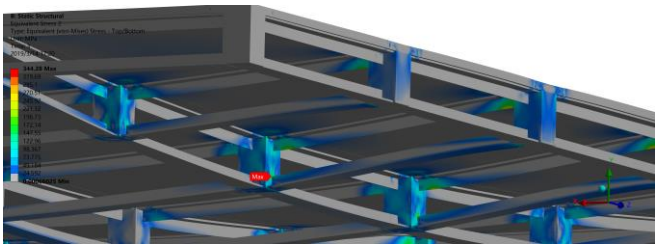

Fig.23 Cloud diagram of some side-span components with equivalent stress

Fig.24 is the equivalent stress cloud diagram after the steel-concrete composite hollow sandwich plate is loaded(17 KN/m^2). From this cloud diagram, the stress distribution of lower steel structure can be obtained. From the overall diagram (Fig.24a), the stress of lower steel hollow beam mainly concentrates in the shear connectors as well as the upper and lower chord section steel near shear connector (green area, 320 Mpa), and at this time,

July - August 2020
ISSN: 0193-4120 Page No. 3624 - 3636

the components have already exceeded the yield stress. The grid element with the maximum stress distribution of shear connector shall be selected, and its stress cloud diagram is observed (Fig.24b). Due to the common action of hollow beam upper chord and concrete plate, the equivalent stress of upper chord steel flange is less than that of lower chord; the upper and lower chords are located at inflection points of grid midspan with smaller stress and strain (gray and light blue areas, 40 MPa). In the construction process, it is safe and reasonable to arrange assembling nodes at grid midspan.

From Fig.24c Cloud diagram of stress at shear connector nodes, the greater stress is mainly at the inter-sectional area of the upper and lower chord section steel and the shear connector, and the maximum stress is at the lap point of upper chord steel flange and shear connector. The main reason lies on that the width of T section steel upper rib flange of test model is less than the width of square steel tube's shear connector. Stress concentration phenomenon exists at the inter-section nodes of two components. Therefore, in actual engineering, the upper and lower chord steel flange and the shear connector should be set as the same width, to enable node compression to be more rational.

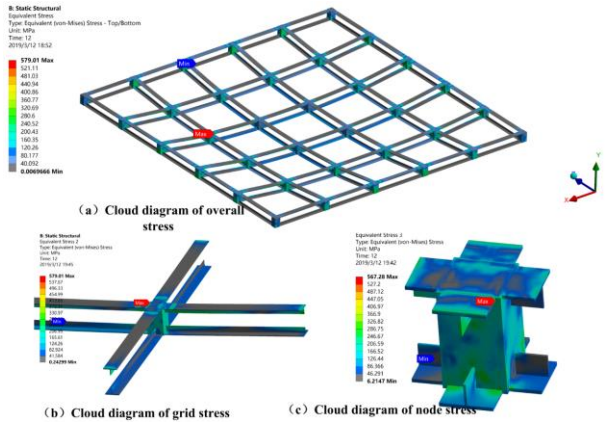

Fig.24 Cloud diagram of equivalent stress after lower steel hollow beam is loaded

Fig.25 is the equivalent stress cloud diagram after the concrete pavement is loaded, with the max. Stress of 307.91 MPa, far more than the ultimate stress of concrete material. This is caused by the contacting between concrete and steel hollow beam grid nodes. The equivalent stress value mainly reflects the node stress of upper chord steel flange contacting the concrete. However, the stress distribution trend of concrete pavement can be obtained from the diagram: the stress distribution of concrete around shear connectors is larger, especially in the concrete area at the pedestal top, so cracks may concentrate in this position when test model is loaded(Fig.13); as the stress in the corner of hollow sandwich plate is smaller, so no crack concentrates in this position, while the stress at concrete plate around neighbouring shear connectors is larger so that through crack produces [19]. In the test, the crack distribution condition of concrete plate agrees with the stress distribution simulated by finite element.

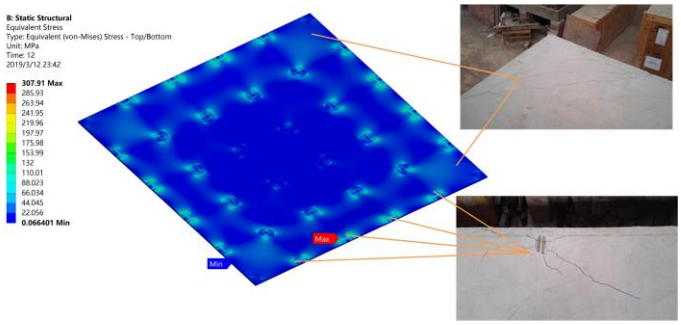

Fig.25 Cloud diagram of equivalent stress after concrete pavement is loaded

5. CONCLUSIONS

This paper took steel-concrete composite hollow sandwich plate as research object, and built a full-scale test model to carry out elastoplastic static properties test, obtained the structural deformation and failure mechanism of steel-concrete composite hollow sandwich plate, and observed the crack development and distribution at concrete pavement, which provides a basis for the design and popularization of steel-concrete composite hollow sandwich plate . The finite element software was adopted to simulate the test process and verified the test phenomenon. The following phenomenon and conclusion were obtained:

July - August 2020
ISSN: 0193-4120 Page No. 3624 - 3636

(1) When the test load reaches to the design load of 4.5 KN/m2, the max. deflection of monitor point 3 is 15.4 mm, i.e. 1/487 of the span, which meets the requirements of design specification. When the load reaches to 17 KN/m2, the ratio of deflection and span at monitor point 3 is 1/82(91.1 mm), the structure has already entered in the yield stage but still does not collapse.

(2) When the test load exceeds the design load, as the load increases, the concrete pavement of hollow sandwich plate gradually show evident cracks, which is symmetrically distributed near shear connector pedestal, and the concrete plate bottom in the middle of hollow sandwich plate grid also shows irregular cracks. When the uniform distributed load reaches to 12KN/m2, at this time, the vertical deflection of steel-concrete composite hollow sandwich plate model quickly rises, ductile failure or bucking failure occurs to the upper and lower chord section steel of the hollow sandwich plate in the first grid, and evident tensile and compressive deformation appears at shear connector pedestal.

(3) At initial loading stage, the strain of monitor points show approximately linear growth with loading steps, and the structure lies in the elastic stage. With increased load, some monitor points yielded, and most yield points at upper and lower chord bars of hollow sandwich plate are located near shear connector. Due to the combined action of concrete plate, the strain value of monitor points at lower chord bar is larger than the monitor value of upper chord bar, the strain of monitor points at upper shear connector is less than that of lower monitor points, and the strain of monitor points in the middle of shear connector is the minimum.

(4) Using the finite element simulation, the results well coincide with test results. This proves that the proposed finite element parameters can well simulate the actual force suffered by the steel-concrete composite hollow sandwich plate.

(5) The upper concrete and lower steel hollow beam of the steel-concrete composite hollow sandwich plate jointly bear force and cooperate to deform, and the overall deformation shows a bowl shape, with significant deformation effect of plate; the steel-concrete composite hollow sandwich plate has a larger ultimate bearing capacity, can completely meet the bearing requirement, and has enough elastoplastic deformation capacity and integrity.

ACKNOWLEDGEMENTS

This work was support by the National Natural Science Foundation of China (51768011), the Guizhou Science Cooperation Foundation [2019]1090, the Guizhou Science Cooperation Foundation [2018]1038 , the Introduction of Talents Research Program of Guizhou University [2016]16.

REFERENCES

[1] Huanqiang Luan, Kejian Ma, Ying Qin, Zhihua Chen and Yanhui Wei (2017) Investigation of the structural of an innovative steel open-web floor system, International Journal of Steel Structures, 17 (4) :1365-1378.

[2] Yong Huang, Weigang Chen and Li Duan. (2011) Experimental study on shear resistance performance of concrete filled steel tube shear block stub columns, Journal of Building Structures, 32 (12) :178-185.

[3] Zhiqiang Bai, Kejian Ma and Wenfeng Liu (2016) Random seismic response of spatial steel-grid box-structure, Journal of Vibration and Shock, 35(14) :163-168.

July - August 2020
ISSN: 0193-4120 Page No. 3624 - 3636

[4] Hongkun Shang, Kejian Ma, Yanhui Wei and Yaqin Lu (2019) Experimental Studies on Shear Resistance Performances for the Shear key of H Shape Steel Spatial Grid Roofs, Latin American Journal of Solids and Structures, 16(5) :1590-1679.

[5] Huanqiang Luan, Kejian Ma, Ying Qin, Xiazhao Li and Zhihua Chen (2016) Investigation of the structural of an innovative steel open-web floor system, International Journal of Steel Structures, 19(2) :353-371.

[6] Jianjun Liu, Kejian Ma, Yanhui Wei, Xiangdong Xu, Jing Chen and Yaqin Lu (2016) Comfort degree analysis and field measurement of single-span multistoried large-span steel grib cassette structural composite open web floors, Building Structure, 46(16) :79-82.

[7] Lu Yang, Yuanqing Wang and Yongjun Shi (2015) Full-Scale Test of Two-Storey Composite Slim Floor under Pseudo-Dynamic and Pseudo-Static Loadings, Advances In Structural Engineering, 18(2) :173-187.

[8] Yunlong Yu, Bo Wei, Yong Yang, Yicong Xue and Hao Xue (2019) Full-Scale Test of Two-Storey Composite Slim Floor under Pseudo-Dynamic and Pseudo-Static Loadings, Advances In Structural Engineering, 22(11) :2406-2417.

[9] Lan Jiang, Kejian Ma, HuagangZhang, Qin Wu, Hongna Lu and Qizhu Yang (2019) Seismic Behavior of Shear Connectors of Steel Vierendeel Sandiwich Plate, Mathematical Problems In Engineer, DIO:10.1155/2019/8047393.

[10] Toi Limazie and Shiming Chen (2015) Numerical procedure for nonlinear behavior analysis of composite slim floor beam, Journal of Constructional Steel Research, 106 :209-219.

[11] Huagang Zhang, Qin Wu, Xiaofei Jia, Hongniao Chen,Kejian Ma, Ming Zao and Guangya Xie (2016) Experimental investigation on compressive strength of cast-in-situ phosphogypsum, Journal of Hunan University (NaturalSciences), 43(3) :127-134.

[12] GB50010-2010, Design Code of Concrete Building, China Architecture & Building Press, Beijing, China, 2010.

[13] Bingqiang Yan, Saijie Che, Dwayne D.Tannant, Fenhua Ren and Peitao Wang (2019) Application of double-yield model in numerical simulation of stability of mining filling body, Arabian Journal of Geosciences, 12(16).

[14] H.P.Mamaghani, T.Usami and E.Mizuno (1996) Inelastic large deflection analysis of structural steel members under cyclic loading, Engineering Structures, 18(9) :659-668.

[15] Li Zhengliang, Zhang Chuntao, Fan Wenliang and Wang Ruheng (2013) Experimental Research on Seismic Behavior of a New Type of Thin-Walled Square Steel Tube Beam-Column Connection, Engineering Mechanics, 30(2) :72-81.

[16] Yin Xu, Shuaiying Wang, Lei Chai and Congcong Luo (2019) Mechanical Performance of Prefabricated External Wall Panel under Horizontal Displacemen, KSCE Journal of Civil Engineering, 22(11) :4519-4529.

[17] Tian hai and He Yiyi (2009) Experiment research and finite element analysis on lateral shearing behavior of ALC spliced-connection wallboard, Journal of building Structures, 30(2) :85-91.

[18] Diego Sosa, Diego Arevalo, E.David Mora, M.Belen Correa, Diego Albuja and Christian Gomez (2017) Experimental and Analytical Study of Slender Reinforced Concrete Shear Wall under Cyclic In-Plane Lateral Load, Mathematical Problems In Engineer, DIO :10.1155/2017/4020563.

[19] Zhipeng Chen, Gang Wu, Decheng Feng and Kejian Ma (2019) Numerical study of the static and dynamic characteristics of reinforced concrete cassette structures for high-rise buildings, Structural Design of Tall and Special Buildings, 28(3), DIO:10.1002/tal.1574.